VIP Solvent-Free Nanofluids

DOI: 10.1002/anie.201208725

Organosiloxane Supramolecular Liquids—Surface-Energy-Driven Phase Transitions**

John Texter, Kejian Bian, Dan Chojnowski, and Joe Byrom*

Dedicated to Bernard Cabane and to Helmut Ringsdorf

Herein, it is shown that autocondensation of organoalkoxysilanes, and subsequent suitable anion exchange, produces core-free and solvent-free nanoparticle nanofluids (organosiloxane supramolecular liquids). Select physical properties of this new class of supramolecular liquids are reported, and we see that classical liquid properties are exhibited but with some distinct differences. Heat capacity anomalies manifested as apparent lambda transitions in excess heat capacity centered around a glass transition (T_g) and around a freezing (melting) transition (T_m) were observed. The T_g-proximal lambda transition is the first experimental realization of an enthalpic phase transition underlying (overlying) a glass transition. The existence of such a connection or coincidence has undergone decades of theoretical conjecture.[1] This anomalous heat capacity spanning the glass transition suggests that some glass transitions may have a thermodynamic basis in addition to a kinetic basis. The second anomaly spanning the melting/freezing range shows that a solid–liquid transition of an amorphous solid can be continuous (in the Ehrenfest[2] sense) rather than first order. Also, this is the first excess enthalpy ever reported for an experimental particulate fluid undergoing a phase transition. The integral enthalpy from these lambda transitions is quantitatively accounted for by the loss of specific surface area of the particles, and the associated surface free energy, upon freezing into an amorphous solid and upon cooling beneath the glass transition temperature.

In the field of materials chemistry there is an increasing focus on hybrid materials composed of diverse nanoobjects in addition to conventional molecules, polymers, metals, and ceramics. Many new materials comprise organic and inorganic components that are solid composites or homogeneous mixtures having synergistic properties. Solvent-free nanofluids are a new class of core/shell particulate liquids; these nanofluids are viscous liquid composites composed of suitably surface-functionalized nanoparticles,[3–5] including protein assemblies such as ferritin that exhibit high thermal stability.[6] Some examples are uncharged,[7,8] but the majority reported to date may be viewed as supramolecular ionic liquids.[9] The preparation of such nanofluids is in its initial stages, but applications for producing new materials include carbon black fluids,[10] carbon nanotube fluids,[11] CO_2 absorbents,[12] and novel resins wherein the reactive nanofluids can increase toughness without imparting brittleness.[13]

Our synthesis was motivated by analytical ultracentrifugation measurements of a nanosilica-core nanofluid functionalized on the surface with trimethoxysilane (Scheme 1) and similarly ion exchanged. Those measurements showed that in addition to the expected silica-core nanofluid, a very high molecular weight impurity of lower density was also present. We then hypothesized that autocondensation of this same silane may also lead to nanofluids. Our two-step synthesis (Scheme 1) yields nanofluid organosiloxane particles with nominal $[C_{81}H_{156}NO_3S(SiO_{[2>x>3/2]})]_y$ stoichiometry, and with units tied together by trigonal (Q) and ladder (T) type connections (see the Supporting Information).[14] The stoichiometric inequality may be appreciated by realizing that 3/2 would be obtained if all siloxy bonds condensed with others and that isolated hydroxy or methoxy groups contribute to x rising above 3/2. The $x = 2$ limit can only be obtained in the case of amorphous or crystalline silica formation with negligible isolated hydroxy groups in the bulk. The resulting nanofluid is thermally robust (TGA), and the synthetic reproducibility was supported by differential scanning calo-

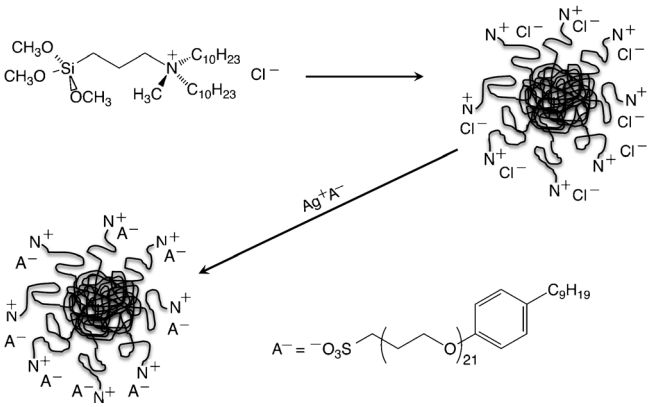

Scheme 1. Condensation of trimethoxysilane to produce a nanoparticulate chloride salt and then subsequent anion exchange of the chloride with a soft and bulky sulfonate to produce the nanofluid. The AgCl is removed by centrifugation.

[*] Prof. Dr. J. Texter, Dr. K. Bian, D. Chojnowski, J. Byrom
School of Engineering Technology, Eastern Michigan University
Ypsilanti, MI 48197 (USA)
E-mail: jtexter@emich.edu

[**] Discussions with Austen Angell and Ian Hodge about these data and glass transitions are gratefully acknowledged. We thank Antje Völkel of the Max Planck Institute for Colloids and Interfaces (Potsdam), for analytical ultracentrifugation and Beatrice Benhamidi for surface-tension measurements. This work was substantially supported by AFOSR Grant No. FA9550-08-1-0431.

Supporting information for this article is available on the WWW under http://dx.doi.org/10.1002/anie.201208725.

rimetry (DSC) of several batches (see the Supporting Information).

By varying the scan rate from 20 °C min^{-1} to 2 °C min^{-1} (see the Supporting Information), we found this nanofluid exhibits classical thermal properties with hysteresis in melting and solidification and a glass transition that is visible on heating and cooling over −61 to −65 °C. The data obtained at a scan rate of 20 °C min^{-1} (0.33 K s^{-1}) showed that this rate is fast enough to almost completely quench the liquid nanofluid into a supercooled glass with almost no heat released. The enthalpy flow from the glass transition is very well defined on cooling and on heating. Upon heating just above the glass transition, a solidification exotherm appears that transforms into a melting endotherm with increasing temperature. At the slower scan rate of 2 °C min^{-1} (0.033 K s^{-1}) nearly all of the nanofluid freezes without forming a glass.

The rheology mirrors the DSC results. A deviation from the results of typical classical liquids is the overall width of approximately 47 °C in the hysteresis of the freezing and melting processes. Averaging the crossover temperatures on heating and cooling we obtain −1 °C as an estimate of T_m. The viscosity varies from 2.4 Pa s at 30 °C to 0.17 Pa s at 100 °C to 0.09 Pa s at 150 °C. These values are similar to those found for viscous fluids such as honey and olive oil. The Arrhenius behavior of the viscosities (see the Supporting Information), however, deviates from classical liquid behavior.

The manner in which such deviations manifest themselves has given rise to the classification of liquids as either strong or fragile.[1c,15] Liquids exhibiting non-Arrhenius behavior in viscosity and/or relaxation times are termed fragile. Amorphous materials often exhibit high- and low-temperature activation energies, and this nanofluid does as well. A high-temperature activation energy of 12.1 kJ mol^{-1} and a lower temperature (30 to 80 °C) activation energy of 38.1 kJ mol^{-1} yield a Doremus fragility ratio of 3.1, thus qualifying this nanofluid as a fragile liquid.[16] The value of the activation energy at the lower temperature is only 20–30 % higher than values measured for ionic liquids at room temperature,[17a] and the values for self-diffusion activation in 250–1000 Da polyisoprene melts come between these values.[17b] On cooling, the inverse temperature dependence of the magnitude of the complex viscosity, calculated from the moduli of Figure 1, similarly shows that the viscosity overall is not Arrhenius prior to the onset of freezing with the diverging viscosity.

Density measurements were made (see the Supporting Information) over the −25 to 90 °C interval. They show that the freezing and melting transitions of this nanofluid are not first order processes, but are continuous (second order) phase transitions. Also with very slow changes in temperature, there is a very wide hysteresis from −22 to 25 °C, similar to the rheology hysteresis illustrated in Figure 1, where a 3 °C min^{-1} scan rate was used. It will be useful in the future to analyze these materials in greater detail to determine what the density is as a function of diameter at a particular temperature, or what the density–temperature behavior is at a given particle diameter.

The TEM in Figure 2 shows that the nanoparticles are polydisperse in size; a few examples appear to have a dimension larger than 10 nm. A conjoined droplet (Figure 2; halfway up on the left-hand side) appears to be almost 20 nm in length, and particles as small as 2 nm appear to be present. The shapes evident in Figure 2 vary from circular to square and from oval to rectangular. We believe this variability emanates from shape distortions induced by the proximal menisci. Some regions exhibit distorted hexagonal packing and others exhibit apparent rectangular packing. The interparticle menisci visible in Figure 2 suggest these particles are not hard spheres, but soft and deformable by the interparticle capillary forces experienced during their deposition from methanol solution. Their partial solvent miscibility and deformability evident in the TEM suggest that these particles interact through a very soft and repulsive interparticle potential and are osmotic spheres, wherein the counterions are osmotically trapped.[18,19] These osmotic spheroids constitute the second reported example of such objects. A nanogel/nanolatex that coalesces upon drying (not a nanofluid) was recently cited[20] as the first experimentally realized example of osmotic spheres.

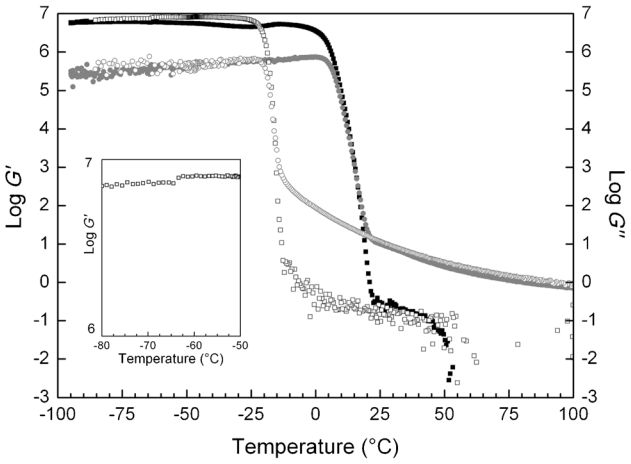

Figure 1. Rheology of nanofluid I. Storage (G′; cooling □; heating ■) and loss (G″; cooling ○; heating ●) moduli have units of Pa. The scan rate was 3 °C min^{-1}. The inset illustrates the step function drop in storage modulus approximately at the T_g at −64 °C.

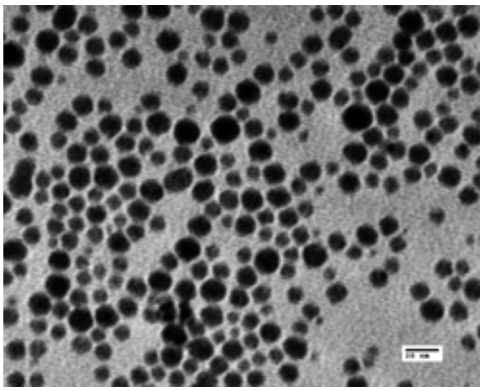

Figure 2. TEM of nanofluid deposited from CH_3OH solution at room temperature. The variability in interparticle menisci illustrates the deformability of nanofluid nanoparticles. Scale bar: 20 nm.

Image analysis of about 11 000 particles done under the assumption of effective particle sphericity yielded monomodal particle size distributions (see the Supporting Information) with a number average diameter of 9.1 nm and a volume average diameter of 11.9 nm. The distributions and moments represent upper bounds. At 25 °C the neat fluid has a density of 1.066 g cm^{-3}. If we assume $x \approx 1.75$, the formula weight of this material is about 1610 Da; 1221 Da (76 %) of this amount is attributed to the sulfonate anion, A^-. At the number average diameter of 9.1 nm, $y \approx 154$; at the weight average diameter of 11.9 nm, $y \approx 344$. There appear to be some very small particles at 3 nm diameter ($y \approx 6$) and even smaller. These smallest particles most likely correspond to multicyclic structures such as octahedral and cubic closed ring systems (see the Supporting Information).

Calculation of first and second moments over these distributions yielded computed polydispersities of 30 %. These polydispersities are important as they affect equations of state, phase diagrams, and whether or not a first order phase transition between liquid and solid may exist.[21] A mean-field study indicates that sufficient polydispersity in hard-sphere systems prevents crystallization.[22] If these nanofluid particles were hard spheres, statistical studies rule out the possibility of crystallization when the polydispersity exceeds 8–12 %. A polydispersity of 30 % perhaps is enough to preclude the possibility of crystallization (as a single phase) in view of the number of very small and very large particles that would create volume-based defects. Our conclusion of continuous freezing and melting is consistent with such a polydisperse material.

Heat capacity measurements determined by a modulated (1 °C/100 s) quasi-isothermal method are illustrated in Figure 3 for three separate preparations of this nanofluid. Surprisingly, lambda transitions superimposed on a larger background heat capacity appear to span both the glass transition and melting–freezing intervals. Such lambda transitions are named for the shape observed in heat capacity measurements, and are continuous in nature rather than first order. The base of the illustrated lambda transition for melting–freezing spans essentially the same 43–45 °C interval exhibited by the hysteresis seen in the rheology and the density plots. It is unequivocal, therefore, that the melting–freezing transition is a continuous (or second order) transition. In the past amorphous solid materials have been referred to as glasses,[23] but this usage is inappropriate when also trying to discuss glasses obtained by temperature quenching processes.

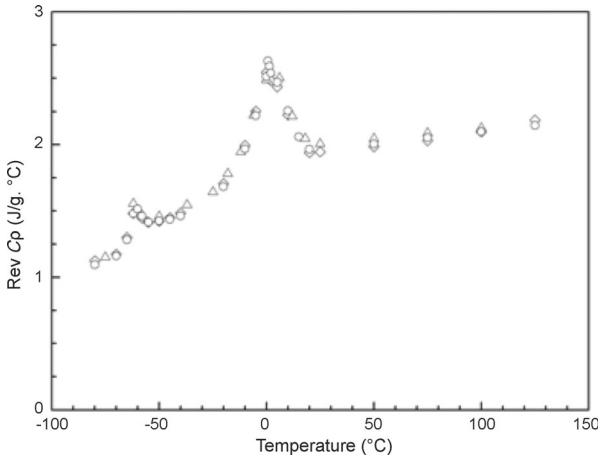

Figure 3. Reversible heat capacity measurements of nanofluid batches I (○), II (△), and III (◇) determined by modulated DSC. Data points were generated sequentially from higher to lower temperatures within each data set. Individual points were obtained by averaging values obtained at a given point in the data set over an approximately 10 min period after temperature quasi-equilibration while modulating the temperature at 1 °C/100 s.

The lambda-shaped transition observed spanning the glass transition interval, ca. 2.2 J g^{-1} in integral excess heat capacity, is of particular interest because, as Jäckle has observed, "the idea of a phase transition underlying a glass transition can only be considered as a theoretical speculation",[24] and later it was reiterated that "the possible linkage between the glass transition and some kind of phase-transition is one of the most debated problems in the theory of liquid and glassy systems".[1] To the best of our knowledge an experimentally observed coincidence of an enthalpic phase transition with a glass transition has heretofore not been reported for any material. These modulated DSC measurements unequivocally demonstrate the existence of a thermodynamic transition occurring over this T_g interval range. A recent analysis[25] of the $Fe_{50}Co_{50}$ superlattice illustrated a case wherein the low-temperature tail of a lambda (order–disorder) transition overlaps a T_g.

The polydispersity of this supramolecular nanofluid system appears to frustrate[26] the formation of a single and homogeneous crystalline state as was previously shown theoretically for hard spheres. Such frustration, in two dimensions, was beautifully demonstrated by Antonietti and co-workers using polydisperse polystyrene nanogels with examples of both Zenon and Apollonian close packing.[27]

The rheology and viscosity divergences on cooling and heating unequivocally match what is required of a freezing–melting order–disorder transition, and the DSC data unequivocally demonstrate these phase transitions as enthalpic (and not hard sphere). These spheroidal nanoparticles appear to be soft spheres, not hard spheres, consistent with the concept of osmotic spheres[18] (when dissolved in solvent), wherein the counterions are trapped within and around the nanofluid particles.

The impact of size polydispersity on hard-sphere fluids has been shown to lead to multiphase domains comprising multiple separate crystalline phases in coexistence with one another and with a fluid phase.[28] Our density data were obtained while simultaneously recording photographs of the U-tube and its contents, and these photos (see the Supporting Information) demonstrate the formation of light-scattering particles (possibly crystals) in coexistence with a much more transparent solid phase. The net composition of these coexisting phases is not known, but the analogy with polydisperse hard-sphere theory is very strong. We therefore believe this intermediate amorphous solid phase comprises coexisting aggregate (most likely crystalline) and amorphous phases as the phase separation is unambiguous. The exo-

therms at −40 °C upon warming above the T_g at −20 and −15 °C min^{-1} show that this rubbery state gains sufficient free volume for nanofluid nanoparticle spatial reorganization and condensation.

Here we are providing soft nanofluids without any added solvent that exhibit non-Arrhenius fragile behavior. In this solvent-free nanofluid system fragility appears to be determined similarly to molecular liquids, as these supramolecular nanofluids are soft and liquid, contrary to some generalizations made for colloidal systems.[29] The main differences between molecular liquids and these nanofluids are in length scale and polydispersity. The latter frustrates formation of a homogeneous crystalline solid phase.

The precedent for solvent-free nanofluids exhibiting viscous flow appears to be polydisperse cross-linked polystyrene nanogels synthesized and characterized by Antonietti and co-workers.[30] Polystyrene nanogels in the 10–100 nm diameter range were prepared by microemulsion polymerization and were solid powders at room temperature after surfactant removal and isolation. However, particle ensembles essentially less than 20 nm in diameter exhibited viscous flow at 150 °C. Although the zero shear viscosities were 10^3–10^8 greater than that (0.067 Pa s) which we report at 150 °C (see the Supporting Information), it is clear that solvent-free nanoparticle-based fluids may have diverse origins in composition and interparticle interaction. Associated solid–liquid transition characteristics were not reported,[30] but the experimental accessibility of such systems makes their further study highly desirable.

The onset of freezing is dependent on the cooling rate, but a supercooled glass is obtained from this nanofluid at the very slow cooling rate of 0.33 K s^{-1}. This aspect will make structural studies of this nanofluid glass very accessible. The possibility of polymorphism suggests that the nature of the solid state between the onset of freezing (T_m) and the T_g may be very interesting, once sufficient structural data become available.

The integral excess enthalpy associated with the freezing–melting lambda transition (Figure 3) is about 16.8 J g^{-1}. The entropy per gram for a fluid–solid transition is of the order of Nk, where N is the particle number density and k is Boltzmann's constant.[31] From the experimental density of 1.066 g cm^{-3} at the onset of freezing (24 °C) and the particle number density of 2.1×10^{18} particles g^{-1} calculated from the number frequency distributions, we see that $T\Delta S \approx 0.01$ J g^{-1} and is negligible in comparison to the enthalpy term. The free energy associated with this freezing transition can be independently approximated by the loss of specific surface area multiplied by the surface energy (tension). If we assume the absence of free volume from interstices between particles after freezing, the surface area lost on freezing can be estimated from the specific surface to volume ratio calculated from the $\langle 6/d \rangle$ moment of the number-frequency particle-size distribution as 7.32×10^6 cm^{-1}. When divided by the density at 24 °C, 6.87×10^6 cm^2 g^{-1} is obtained as the specific surface area of the nanofluid. Pendent drop measurements of surface tension yielded a surface energy of 28 erg cm^{-2}. This value agrees well with the correlation of surface energy with molar volume presented by Maroncelli and co-workers.[32] The surface free energy (assuming the macroscopic values apply to the nanoparticles) is then 19.1 J g^{-1}. The experimental enthalpy for both transitions, therefore, can be explained quantitatively by the loss of specific surface area on condensation of the particles into an amorphous solid state accompanying loss of interparticle interstices.

The lambda transition overlying the T_g was obtained by cooling the sample very slowly, whereby little if any of the glass formed at a cooling rate of 0.33 K s^{-1}. This lambda transition, therefore, is a property of the amorphous solid, but a kinetic glass transition is produced over the same temperature interval by supercooling the liquid. It has been asserted that the possibility of crystallization (aggregation) within a glass phase cannot be discounted,[33] and we hypothesize this lambda transition emanates from loss of specific surface area not extinguished in the higher lying freezing transition. We cannot yet distinguish if supramolecular degrees of freedom between and/or within these nanoparticles may be the source of this rare coincidence, but we believe a more definitive connection between this glass and associated lambda transitions will be revealed by further experimentation.

The size polydispersity in this nanofluid may provide further insight into the role of free volume in molecular and supramolecular liquids and fodder for modeling and understanding the structure of liquids. The coexistence demonstrated by the precipitation within the amorphous solid (see the Supporting Information) state while cooling through the melting/freezing interval finds support in the moment-free energy theory developed for hard spheres,[28] except in this case the freezing (lambda) transition proves these processes are enthalpic (rather than hard sphere). We expect such organosiloxane nanoparticles to be synthetically tunable for experimentally creating systematic variations in interparticle potentials and in interparticle (interstice) free volumes. We expect such tuning to provide designer control of thin-film and bulk-phase transitions and enhanced understanding of particle-based association and coalescence phenomena.

Experimental Section

Trimethoxysilane [*N*,*N*-didecyl-*N*-methyl-*N*-(3-trimethoxysilylpropyl) ammonium chloride] was condensed in methanol with a small amount of water over a two day period. After harvesting the chloride salt by centrifugation and drying, anion exchange of the chloride was carried out by preparative potentiometric titration with the silver sulfonate [poly(ethylene glycol)-4-nonylphenyl 3-sulfopropyl ether silver salt] to produce the product. After suitable dialysis, lyophilization, and drying, a solvent-free nanofluid of moderate viscosity was obtained. A full account of the synthesis procedures is given in the Supporting Information.

Received: October 31, 2012
Published online: January 22, 2013

Keywords: glass transition · glasses · heat capacity · lambda transition · phase transitions

[1] a) L. Ferrari, G. Russo, *J. Phys. Condens. Matter* **1993**, *5*, 5525–5542; b) C. A. Angell, K. L. Ngai, G. B. McKenna, P. F. McMil-

lan, S. W. Martin, *J. Appl. Phys.* **2000**, *88*, 3113 – 3157; c) P. G. Debenedetti, F. Stillinger, *Nature* **2001**, *410*, 259 – 267.
[2] G. Jaeger, *Arch. Hist. Exact Sci.* **1998**, *53*, 51 – 81.
[3] A. B. Bourlinos, R. Herrera, N. Chalkias, D. D. Jiang, Q. Zhang, et al., *Adv. Mater.* **2005**, *17*, 234 – 237.
[4] a) S. C. Warren, M. J. Banholzer, L. S. Slaughter, E. P. Giannelis, F. J. DiSalvo, U. B. Wiesner, *J. Am. Chem. Soc.* **2006**, *128*, 12074 – 12075; b) R. Rodriguez, R. Herrera, L. A. Archer, E. P. Giannelis, *Adv. Mater.* **2008**, *20*, 4353 – 4358.
[5] J. L. Nugent, S. S. Moganty, L. A. Archer, *Adv. Mater.* **2010**, *22*, 3677 – 3680.
[6] A. W. Perriman, H. Coelfen, R. W. Hughes, C. L. Barrie, S. Mann, *Angew. Chem.* **2009**, *121*, 6360 – 6364; *Angew. Chem. Int. Ed.* **2009**, *48*, 6242 – 6246.
[7] O. Thompson Mefford, M. L. Vadala, J. D. Goff, M. R. J. Carroll, R. Mejia-Ariza, B. L. Caba, T. G. St. Pierre, R. C. Woodward, R. M. Davis, J. S. Riffle, *Langmuir* **2008**, *24*, 5060 – 5069.
[8] T. Nakanishi, *Chem. Commun.* **2010**, *46*, 3425 – 3436.
[9] S. S. Moganty, N. Jayaprakash, J. L. Nugent, J. Shen, L. A. Archer, *Angew. Chem.* **2010**, *122*, 9344 – 9347; *Angew. Chem. Int. Ed.* **2010**, *49*, 9158 – 9161.
[10] Q. Li, L. Dong, J. Fang, C.-X. Xiong, *ACS Nano* **2010**, *4*, 5797 – 5806.
[11] Y. Lei, C.-X. Xiong, H. Guo, J.-L. Yao, L. Dong, X.-H. Su, *J. Am. Chem. Soc.* **2008**, *130*, 3250 – 3257.
[12] K.-Y. A. Lin, A.-H. A. Park, *Environ. Sci. Technol.* **2011**, *45*, 6633 – 6639.
[13] J. Texter, Z. Qiu, R. Crombez, J. Byrom, W. Shen, *Polym. Chem.* **2011**, *2*, 1778 – 1787.
[14] a) R. Joseph, S. Zhang, W. T. Ford, *Macromolecules* **1996**, *29*, 1305 – 1312; b) F. Bauer, H.-J. Gläsel, U. Decker, H. Ernst, A. Freyer, E. Hartmann, V. Sauerland, R. Mehnert, *Prog. Org. Coat.* **2003**, *47*, 147 – 153.
[15] C. A. Angell, *Science* **1995**, *267*, 1924 – 1935.
[16] a) M. I. Ojovan, *Adv. Cond. Matt. Phys.* **2008**, 817829; b) R. H. Doremus, *J. Appl. Phys.* **2002**, *92*, 7619 – 7629.
[17] a) R. E. Baltus, http://people.clarkson.edu/~baltus/RoomTemperature Ionic Liquids.pdf, downloaded 30 October 2012; b) V. A. Harmandaris, M. Doxostakis, V. G. Mavrantzas, D. N. Theodorou, *J. Chem. Phys.* **2002**, *116*, 436 – 446.
[18] P. Pincus, *Macromolecules* **1991**, *24*, 2912 – 2919.
[19] A. Jusufi, C. N. Likos, H. Löwen, *J. Chem. Phys.* **2002**, *116*, 11011 – 11027.
[20] D. England, N. Tambe, J. Texter, *ACS Macro Lett.* **2012**, *1*, 310 – 314.
[21] S.-E. Phan, W. B. Russel, J. Zhu, P. M. Chaikin, *J. Chem. Phys.* **1998**, *108*, 9789 – 9795.
[22] P. Bartlett, P. B. Warren, *Phys. Rev. Lett.* **1999**, *82*, 1979 – 1982.
[23] J. H. Gibbs, E. H. DiMarzio, *J. Chem. Phys.* **1958**, *28*, 373 – 383.
[24] J. Jäckle, *Rep. Prog. Phys.* **1986**, *49*, 171 – 231.
[25] S. Wei, Y. Gallino, R. Busch, C. A. Angell, *Nat. Phys.* **2011**, *7*, 178 – 182.
[26] P. Yunker, Z. X. Zhang, A. G. Yodh, *Phys. Rev. Lett.* **2010**, *104*, 015701.
[27] M. Antonietti, J. Hartmann, M. Neese, U. Seifert, *Langmuir* **2000**, *16*, 7634 – 7639.
[28] M. Fasolo, P. Sollich, *Phys. Rev. Lett.* **2003**, *91*, 068301.
[29] C. A. Angell, K. Ueno, *Nature* **2009**, *462*, 45 – 46.
[30] M. Antonietti, T. Pakula, W. Bremser, *Macromolecules* **1995**, *28*, 4227 – 4233.
[31] W. G. Hoover, F. H. Ree, *J. Chem. Phys.* **1968**, *49*, 3609 – 3617.
[32] H. Jin, B. O'Hare, J. Dong, S. Arzhantsev, G. A. Baker, J. F. Wishart, A. J. Benesi, M. Maroncelli, *J. Phys. Chem. B* **2008**, *112*, 81 – 92.
[33] E. Zaccarelli, C. Valeriani, E. Sanz, W. C. K. Poon, M. E. Cates, et al., *Phys. Rev. Lett.* **2009**, *103*, 135704.

